

CCLF: A Contrastive-Curiosity-Driven Learning Framework for Sample-Efficient Reinforcement Learning

Chenyu Sun^{1,2}, Hangwei Qian^{2,3} * and Chunyan Miao^{1,2} *

¹Alibaba-NTU Singapore Joint Research Institute, Nanyang Technological University

²School of Computer Science and Engineering, Nanyang Technological University

³Lund University

chenyu002@e.ntu.edu.sg, hangwei.qian@math.lth.se, ascymiao@ntu.edu.sg

Abstract

In reinforcement learning (RL), it is challenging to learn directly from high-dimensional observations, where data augmentation has recently been shown to remedy this via encoding invariances from raw pixels. Nevertheless, we empirically find that not all samples are equally important and hence simply injecting more augmented inputs may instead cause instability in Q-learning. In this paper¹, we approach this problem systematically by developing a model-agnostic Contrastive-Curiosity-driven Learning Framework (CCLF), which can fully exploit sample importance and improve learning efficiency in a self-supervised manner. Facilitated by the proposed contrastive curiosity, CCLF is capable of prioritizing the experience replay, selecting the most informative augmented inputs, and more importantly regularizing the Q-function as well as the encoder to concentrate more on under-learned data. Moreover, it encourages the agent to explore with a curiosity-based reward. As a result, the agent can focus on more informative samples and learn representation invariances more efficiently, with significantly reduced augmented inputs. We apply CCLF to several base RL algorithms and evaluate on the DeepMind Control Suite, Atari, and MiniGrid benchmarks, where our approach demonstrates superior sample efficiency and learning performances compared with other state-of-the-art methods.

1 Introduction

Despite the success of reinforcement learning (RL), extensive data collection and environment interactions are still required to train the agents [Laskin *et al.*, 2020b]. In contrast, human beings are capable of learning new skills quickly and generalizing well with limited practice. Therefore, bridging the gap of sample efficiency and learning capabilities between machine and human learning has become a main challenge in the RL community [Rakelly *et al.*, 2019; Schwarzer *et al.*, 2020; Yarats *et al.*, 2021b; Malik *et al.*, 2021; Sun *et al.*, 2022].

This challenge is particularly vital in learning directly from raw pixels. More recently, data augmentation methods are leveraged to incorporate more invariances, promote data diversity, and thereby enhance representation learning [Laskin *et al.*, 2020b; Yarats *et al.*, 2020; Yarats *et al.*, 2021a]. Ideally, injecting a larger number of augmented samples should lead to a better model with invariances. Nevertheless, a noticeable trade-off is the computational complexity introduced. What’s worse, simply increasing the number of augmented inputs may alter the semantics of samples, which has been empirically shown in our experimental results. Moreover, the samples used for data augmentation are uniformly drawn from the replay buffer [Laskin *et al.*, 2020a; Laskin *et al.*, 2020b; Yarats *et al.*, 2020; Yarats *et al.*, 2021a], which is inefficient as they are not equally important to learn. These assumptions deviate from human-like intelligence, where humans can learn efficiently by curiously focusing on novel knowledge and revisiting old knowledge less frequently. Therefore, replaying the most under-explored experiences and selecting the most informative augmented inputs are the keys to improving sample efficiency and learning capability.

To tackle these challenges, we propose a Contrastive-Curiosity-driven Learning Framework (CCLF) by introducing contrastive curiosity into four important components of RL including experience replay, training input selection, learning regularization, and task exploration without much computational overhead. Inspired by the psychological curiosity that can be externally stimulated, encompassing complexity, novelty, and surprise [Berlyne, 1960; Spielberg and Starr, 2012; Liquin and Lombrozo, 2020], we define the contrastive curiosity based on the surprise conceptualized by the agent’s internal belief towards the augmented inputs. The internal belief is modeled by reusing the contrastive loss term in CURL [Laskin *et al.*, 2020a], which can quantitatively measure the curiosity level without introducing any additional network architecture. With the proposed contrastive curiosity, agents can sample more under-explored transitions from the replay buffer, and select the most informative augmented inputs to encode invariances. This process can significantly reduce the amount of data used in RL without sacrificing the invariances. Thereafter, CCLF further utilizes the contrastive curiosity to regularize both Q-function and encoder by concentrating more on the surprising inputs, and intrinsically rewards agents for exploring under-learned observations.

*Co-corresponding authors

¹Accepted at IJCAI 2022 under IJCAI-ECAI 2022

Our contribution can be highlighted as follows. 1) We empirically demonstrate that not all samples nor their augmentations are equally important in RL. Thus, agents should learn curiously from the most important ones in a self-supervised manner. 2) A surprise-aroused type of curiosity, namely, contrastive curiosity, is proposed by reusing the representation learning module without increasing the network complexity. 3) The proposed CCLF is capable of improving the sample efficiency and adapting the learning process directly from raw pixels, where the contrastive curiosity is fully exploited in different RL components in a self-navigated and coherent way. 4) CCLF is model-agnostic and can be applied to model-free off-policy and on-policy RL algorithms. 5) Compared to other approaches, CCLF obtains state-of-the-art performance on the DeepMind Control (DMC) suite [Tunyasuvunakool *et al.*, 2020], Atari Games [Bellemare *et al.*, 2013], and Mini-Grid [Chevalier-Boisvert *et al.*, 2018] benchmarks.

2 Related Works

Data Augmentation in Sample-Efficient RL. Data augmentation has been widely applied in computer vision but is only recently introduced in RL to incorporate invariances for representation learning [Laskin *et al.*, 2020b; Yarats *et al.*, 2020; Laskin *et al.*, 2020a]. To further improve the sample efficiency, one approach is to automatically apply the most effective augmentation method on any given task, through a multi-armed bandit or meta-learning the hyper-parameters to adapt [Raileanu *et al.*, 2020]. However, the underlying RL algorithm can become non-stationary and it costs more time to converge. Another approach is to regularize the learning process with observations from different training environments [Wang *et al.*, 2020] or different steps [Yarats *et al.*, 2021a]. By injecting greater perturbations from other tasks and steps, the encoded features and learned policies can become more robust to task invariances. Different from these works, the proposed CCLF primarily focuses on perturbations generated in a single task and step, and selects the most under-learned transition tuples and their augmented inputs. As not all samples nor their augmented inputs are equally important, our work exploits the sample importance to adapt the learning process by concentrating more on under-explored samples. Most importantly, the amount of augmentations can be greatly reduced and the sample efficiency is improved without introducing complicated architectures.

Curiosity-Driven RL. In curiosity-driven RL, agents are intrinsically motivated to explore the environment and perform complex control tasks by incorporating curiosity [Wu and Miao, 2013; Aubret *et al.*, 2019; Sun *et al.*, 2022]. In particular, curiosity is mainly used as a sophisticated intrinsic reward based on state novelty [Bellemare *et al.*, 2016], state prediction errors [Pathak *et al.*, 2017], and uncertainty about outcomes [Li *et al.*, 2021] or environment dynamics [Seo *et al.*, 2021]. Meanwhile, it can also be employed to prioritize the experience replay towards under-explored states [Schaul *et al.*, 2016; Zhao and Tresp, 2019]. However, additional networks are required to model curiosity, which can be computationally inefficient and unstable for high-dimensional inputs with continuous controls. Moreover, none of these works

have yet attempted to improve the sample efficiency and resolve the instability caused by data augmentation. CCFDM [Nguyen *et al.*, 2021] is a concurrent work that incorporates CURL with action embedding and forward dynamics to formulate an intrinsic reward. Different from CCFDM, our framework does not require any additional architecture but only reuses the contrastive term in CURL that predicts more stably. More importantly, the proposed CCLF seamlessly integrates the curiosity mechanism into experience replay, training input selection, learning regularization, and environment exploration to concentrate more on under-learned samples and improve the sample efficiency stably.

3 Background

In this paper, we consider a Markov Decision Process (MDP) setting with the state $s_t \in \mathcal{S}$, the action $a_t \in \mathcal{A}$, the transition probability P mapping from the current state s_t and action a_t to the next state s'_t , and the (extrinsic) reward $r_t^e \in \mathcal{R}$. More details are provided in Appendix A.

Soft Actor-Critic (SAC). SAC [Haarnoja *et al.*, 2018] is an off-policy model-free algorithm that learns a stochastic policy π_ψ (actor) with state-action value functions Q_{ϕ_1}, Q_{ϕ_2} (critics), and a temperature α by encouraging exploration through a γ -discounted maximum-policy-entropy term. However, agents are often required to learn directly from high-dimensional observations $o_t \in \mathcal{O}$ rather than states s_t in practice. In this paper, we demonstrate our framework mainly using SAC with raw pixel inputs as the base algorithm.

Contrastive Unsupervised RL (CURL). CURL [Laskin *et al.*, 2020a] utilizes data augmentation and contrastive learning to train an image encoder $f_\theta(o)$ in a self-supervised way, imposing an instance discrimination between similar (+) and dissimilar (−) encoded states. Given a batch of visual observations o , each is augmented twice and encoded into a query $q = f_\theta(o_q)$ and a key $k = f_\theta(o_k)$. The key encoder f_θ is a momentum-based moving average of the query encoder f_θ to ensure consistency and stability, and f_θ is learned by enforcing q to match with k^+ while keeping far apart from k^- .

Data Regularized Q-Learning (DrQ). Based on SAC settings, DrQ [Yarats *et al.*, 2020] incorporates optimality invariant image transformations to regularize the Q-function, improving robust learning directly from raw pixels. Let $g(o)$ represent the random image crop augmentation on observations o . It should ideally preserve the Q-values s.t. $Q(o, a) = Q(g_i(o), a), \forall o \in \mathcal{O}, a \in \mathcal{A}, i = 1, 2, 3, \dots$. DrQ then applies data augmentation to each transition tuple $\tau_t = (o_t, a_t, r_t^e, d_t, o'_t)$ that is uniformly sampled from the replay buffer \mathcal{B} , where d_t is the done signal. With K augmented next observations $g_k(o'_t)$ and M augmented current observations $g_m(o_t)$, the critic Q_ϕ can be regularized by averaging over M augmented inputs from o_t ,

$$\mathcal{L}_Q(\phi) = \mathbb{E}_{\tau \sim \mathcal{B}} \left[\frac{1}{M} \sum_{m=1}^M \left(Q_\phi(g_m(o_t), a_t) - (r_t^e + \gamma(1 - d_t)\mathcal{T}_t) \right)^2 \right] \quad (1)$$

where \mathcal{T}_t is the soft target value and it can also be regularized by averaging over K augmented inputs from o'_t ,

$$\mathcal{T}_t = \frac{1}{K} \sum_{k=1}^K [\min_{i=1,2} Q_{\phi_i}(g_k(o'_t), a'_k) - \alpha \log \pi_\psi(a'_k | g_k(o'_t))]. \quad (2)$$

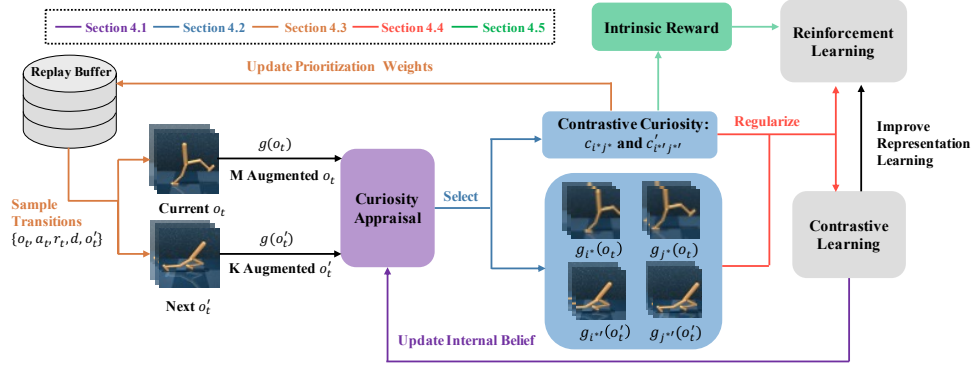


Figure 1: Contrastive-Curiosity-driven Learning Framework (CCLF): a batch of transitions are sampled w.r.t. their prioritization weights. Image augmentation is performed to obtain M augmented o_t and K augmented o_t' . The curiosity appraisal module quantitatively evaluates the contrastive curiosity and selects the two most informative inputs for both current and next observations. More importantly, the contrastive curiosity is simultaneously utilized to update the prioritization weights, construct an intrinsic reward, and adaptively regularize the contrastive learning and Q-learning modules. The contrastive learning module improves the representation learning and updates the agent’s internal belief.

4 The Proposed CCLF

Contrastive-Curiosity-driven Learning Framework (CCLF) extends the model-free RL to further improve sample efficiency when learning directly from the raw pixels. In particular, it fully exploits sample importance for agents to efficiently learn from the most informative data. Firstly, we repurpose the contrastive term in CURL [Laskin *et al.*, 2020a] without additional architectures to quantify the contrastive curiosity (Section 4.1). Subsequently, this contrastive curiosity is coherently integrated into four components to navigate RL with minimum modification: augmented input selection (Section 4.2), experience replay (Section 4.3), Q-function and encoder regularization (Section 4.4), and environment exploration (Section 4.5), as illustrated in Figure 1. Without loss of generality, we apply CCLF on the state-of-the-art off-policy RL algorithm, SAC [Haarnoja *et al.*, 2018] as summarized in Algorithm 1². Extensions on other base algorithms are carried out in Section 5.2 and Appendix B.2 and B.3.

4.1 Contrastive Curiosity

Curiosity can be aroused by an unexpected stimulus that behaves differently from the agent’s internal belief. To quantify such surprise-aroused curiosity, we define the agent’s curiosity c_{ij} by the prediction error of whether any two augmented observations $g_i(o)$, $g_j(o)$ are from the same observation o ,

$$c_{ij} = 1 - \text{IB}(g_i(o), g_j(o)) \in [0, 1] \quad (3)$$

where IB represents agent’s internal belief of whether $g_i(o)$, $g_j(o)$ are augmented (e.g., randomly cropped) from the same o with similar representations. Since the contrastive loss can be viewed as the log-loss of a softmax-based classifier to match a query q with the key k from the same observation in a batch, it becomes a natural choice for measuring agent’s internal belief $\text{IB}(g_i(o), g_j(o)) = \frac{\exp(q^T W k^+)}{\exp(q^T W k^+) + \sum_{l=1}^{B-1} \exp(q^T W k_l^-)}$, where B is the batch size and q is the query encoder $q = f_\theta(g_i(o))$. Moreover, we denote the key encoder $k = f_{\bar{\theta}}(g_j(o))$ as k^+ if its input is the same as that in the query encoder q ; otherwise, we denote it as k^- . An immediate merit is that the

contrastive curiosity does not require any additional architecture or auxiliary loss because IB is updated directly through representation learning in a self-supervised way.

A higher contrastive curiosity value indicates that the agent does not believe q is similar to k^+ or the agent mistakenly matches q with some k^- instead, which ultimately results in a surprise in a self-supervised way. It further implies that the sampled transition tuple contains novel information that has yet been learned by the agent, and the encoder f_θ is not optimal to extract a meaningful state representation from raw pixels. With the proposed contrastive curiosity in-place, we can integrate different curiosity-driven mechanisms in the proposed CCLF to achieve sample-efficient RL, which is discussed in the following sub-sections.

4.2 Curiosity-Based Augmented Input Selection

Although DrQ [Yarats *et al.*, 2020] has shown that increasing $[K, M]$, i.e., the amounts of augmented inputs on next and current observations respectively, can potentially improve agent’s performances through regularized Q-learning, a crucial trade-off is the introduced higher computational complexity. In addition, more augmented data does not necessarily lead to better performance, as data transformations might alter the semantics and result in the counterproductive performance. To tackle these challenges, we aim to select the most informative inputs for the subsequent learning. Without loss of generality, we assume two inputs are selected from M augmented current observations o_t and similarly two are selected from K augmented next observations o_t' in this paper.

It should be noted that there are various ways to select the most informative augmented inputs, where one straightforward way is to select by least overlap in pixels,

$$i^*, j^* = \arg \min \text{Overlap}(g_i(o), g_j(o)) \quad \forall i, j, i \neq j. \quad (4)$$

However, a more human-like way is to select the most representative inputs based on the curious level conceptualized by the internal belief rather than simple visual overlaps. Therefore, we propose to select the augmented inputs that cause highest contrastive curiosity as defined in Eq. (3),

$$i^*, j^* = \arg \max c_{ij} \quad \forall i, j, i \neq j. \quad (5)$$

In this way, the augmented inputs that are most challenging for matching can be curiously identified since they potentially

²Our code is available at <https://github.com/csun001/CCLF>.

contain novel knowledge that has yet been learned; meanwhile, this selection mechanism can help to encode more representative state information from the selected inputs, while the agent’s internal belief can be jointly updated. As a result, an improved encoder that is robust to different views of observations can be trained with fewer inputs, potentially yielding an improvement for the sample efficiency.

4.3 Curiosity-Based Experience Replaying

In the conventional off-policy RL, agents uniformly sample transitions τ from the replay buffer to learn policies. Although they can eventually perform a complex task by repeatedly practicing in a trial-and-error fashion, we hypothesize that a more sample-efficient and generalizable way is to revisit the transitions that are relatively new or different more frequently. Therefore, we prioritize the experience replay by assigning different prioritization weights $w \in [0, 1]$ to all transitions stored in the replay buffer \mathcal{B} . In particular, the prioritization weight is initialized to $w_0 = 1$ for any newly added transition tuple. Thereafter, we propose to update the weights of transitions with the overall contrastive curiosity at each training step s ,

$$w_s = \beta w_{s-1} + \frac{1}{2}(1 - \beta)(c_{i^*j^*} + c'_{i'^*j'^*}) \quad (6)$$

where $\beta \in [0, 1]$ is a momentum coefficient, and $c_{i^*j^*}, c'_{i'^*j'^*}$ are the contrastive curiosity about o and o' respectively. The intuition of the momentum update is to maintain a stable update such that the transitions arousing low curiosity will be gradually de-prioritized for learning. Mathematically, the probability of τ_i to be replayed is $p(\tau_i) = \frac{w_i}{\sum_{n=1}^N w_n}$ and it becomes small only when τ_i has been sampled many times. Hence, more recent and surprising transitions arousing high curiosity can be sampled more frequently to learn.

4.4 Curiosity-Based Regularization

Although agents can benefit from learning the selected complex inputs, it imposes challenges for agents as well, which may cause unstable and poor performances. Hence, it is crucial to adapt the learning process by concentrating more on under-learned knowledge. To achieve this, we propose an adaptive regularization for both Q-function and the observation encoder, guided by the contrastive curiosity in order to learn more from the selected inputs arousing high curiosity. In particular, we modify Eq. (2) and Eq. (1) as

$$\begin{aligned} \mathcal{L}_Q(\phi) &= \mathbb{E}_{\tau \sim \mathcal{B}} [(1 - c_{i^*j^*})\mathcal{E}_{i^*}^2 + c_{i^*j^*}\mathcal{E}_{j^*}^2], \\ \mathcal{T}_t &= (1 - c'_{i'^*j'^*})\mathcal{T}_t^{i'^*} + c'_{i'^*j'^*}\mathcal{T}_t^{j'^*}, \\ \text{where } \mathcal{E}_m &= Q_\phi(g_m(o_t), a_t) - (r_t^e + \gamma(1 - d_t)\mathcal{T}_t), \quad m = i^*, j^*, \\ \text{and } \mathcal{T}_t^k &= \min_{l=1,2} Q_{\bar{\phi}_l}(g_k(o'_t), a'_k) - \alpha \log \pi_\psi(a'_k | g_k(o'_t)), \quad k = i'^*, j'^*. \end{aligned} \quad (7)$$

It is worth noting that this regularized Q-function is rather general to recover other state-of-the-art works as special cases. When all augmented inputs arouse exactly moderate level of curiosity $c_{i^*j^*} = c'_{i'^*j'^*} = \frac{1}{2}$, the proposed regularization is equivalent to DrQ with $[K, M] = [2, 2]$. Moreover, when the agent can perfectly match the two augmented inputs

Algorithm 1 An Implementation of CCLF on SAC

Input: MDP $\tau_t = (o_t, a_t, r_t^e, d_t, o'_t)$, numbers of augmented inputs $[K, M]$, replay buffer \mathcal{B} , training step T , batch size B
Parameter: Observation encoder network θ , actor network ψ , critics networks ϕ_i , temperature coefficient α , and bilinear product weight W

Output: Optimal policy π_ψ^*

```

for  $t = 1$  to  $T$  do
   $a_t \sim \pi_\psi(\cdot | g(o_t))$ 
   $\mathcal{B} \cup (o_t, a_t, r_t^e, d_t, o'_t) \rightarrow \mathcal{B}$  with  $w_t = 1$ 
  Sample a minibatch  $\{(o_l, a_l, r_l^e, d_l, o'_l)\}_{l=1}^B \stackrel{w_l}{\sim} \mathcal{B}$  based
  on the prioritization weight  $w_l$ 
  for each sample  $\tau_l$  in the minibatch do
    Augment  $o_l$  and  $o'_l$  via  $g(\cdot)$  to obtain  $M$  and  $K$  inputs
    Evaluate the contrastive curiosity  $c_{ij}$  by Eq. (3)
    Select  $g_{i^*}(o_l), g_{j^*}(o_l)$  from  $M$  augmented  $o_l$  and se-
    lect  $g_{i'^*}(o'_l), g_{j'^*}(o'_l)$  from  $K$  augmented  $o'_l$  by Eq. (5)
     $r_l = r_l^e + r_l^i$  with  $r_l^i$  from Eq. (9)
    Update  $w_l$  according to Eq. (6)
  end for
  Update critics  $Q_{\phi_i}$  by Eq. (7)
  Update the actor  $\pi_\psi$  and temperature coefficient  $\alpha$ 
  Update encoder  $f_\theta$  and  $W$  by Eq. (8)
   $o_{t+1} = o'_t$ 
end for

```

with no contrastive curiosity $c_{i^*j^*} = c'_{i'^*j'^*} = 0$, it is sufficient to update the Q-function with only one input; when the agent fails to encode any similarity and becomes extremely curious $c_{i^*j^*} = c'_{i'^*j'^*} = 1$, it should focus completely on the novel input instead. Both cases can reproduce the work of RAD [Laskin *et al.*, 2020b]. Most importantly, our proposed Q-function regularization enables the agent to adapt the learning process in a self-supervised way that it is fully controlled by the conceptualized contrastive curiosity to exploit sample importance and stabilize the learning process.

Similarly, we also regularize the representation learning in a curious manner, inspired by the solution to the supervised class imbalance problem. To deal the with training set containing under-represented classes, a practical approach is to inversely weight the loss of each class according to their sizes. We follow this motivation to incorporate the contrastive curiosity $c_{i^*j^*}^b$ about the current observations as the weight for each log-loss class b to update the encoder f_θ ,

$$\mathcal{L}_f(\theta) = - \sum_{b=1}^B c_{i^*j^*}^b \log \frac{\exp(q_b^T W k^+)}{\exp(q_b^T W k^+) + \sum_{l=1}^{B-1} \exp(q_b^T W k_l^-)} \quad (8)$$

where samples arousing high contrastive curiosity will be considered as under-represented classes and therefore agents need to adaptively pay more attention during the representation learning by optimizing f_θ . Meanwhile, agents also jointly re-calibrate a proper internal belief by updating W .

4.5 Curiosity-Based Exploration

Intrinsic rewards can motivate agents to explore actively [Sun *et al.*, 2022], improving the sample efficiency in the conventional RL. While SAC alone can be viewed as the entropy

100K Step Scores	SAC-Pixel	CURL	DrQ	CURL+	CURL++	Select	Select+	CCLF
Finger, Spin	230±194	686±113	784±173	780±96	735±120	699±138	768±90	944±42
Cartpole, Swingup	237±49	524±179	675±174	694±87	665±122	624±182	561±181	799±61
Reacher, Easy	239±183	566±226	682±86	541±190	479±216	646±171	616±284	738±99
Cheetah, Run	118±13	286±65	332±36	302±50	264±53	251±26	265±69	317±38
Walker Walk	95±19	482±237	492±267	484±61	504±142	453±91	408±170	648±110
Ball in Cup, Catch	85±130	667±197	828±131	687±260	728±143	732±223	739±132	914±20
500K Step Scores	SAC-Pixel	CURL	DrQ	CURL+	CURL++	Select	Select+	CCLF
Finger, Spin	346±95	783±192	803±198	855±164	838±164	803±167	879±153	974±6
Cartpole, Swingup	330±73	847±28	858±19	853±22	852±17	855±26	837±38	869±9
Reacher, Easy	307±65	956±40	939±44	933±62	937±40	939±78	906±80	941±48
Cheetah, Run	85±51	440±144	536±115	518±24	495±97	417±59	470±78	588±22
Walker Walk	71±52	928±26	887±126	916±27	914±24	921±27	850±64	936±23
Ball in Cup, Catch	162±122	956±14	956±14	951±19	956±8	949±21	949±24	961±9

Table 1: Performance scores (mean & standard deviation) on DMC evaluated at 100K and 500K environment steps. CCLF outperforms other approaches on 5 out of 6 tasks in both sample efficiency (100K) and asymptotic performance (500K) regimes, across 6 random seeds.

maximization of agent’s actions intrinsically, in the proposed CCLF, we explicitly define an intrinsic reward proportional to the average contrastive curiosity about o_t and o'_t ,

$$r_t^i = \lambda \exp(-\eta t) \frac{r_{max}^e c_{i^*j^*} + c'_{i^*j^*}}{r_{max}^i} \quad (9)$$

where λ is a temperature coefficient, η is a decay weight, t is the environment step, r_{max}^e and r_{max}^i are respectively the maximum extrinsic and intrinsic rewards over step t .

With the proposed r_t^i to supplement r_t^e in Eq. (7), agents can be encouraged to explore the surprising states that arouse high contrastive curiosity substantially. In particular, higher r_t^i rewards agents for exploration when different views of the same observations produce inconsistent representations. Meanwhile, r_t^i is decayed with respect to the environment step t to ensure the convergence of policies. As the extrinsic reward r^e differs across different tasks, the normalization is performed to balance r^e and r^i . This formulation is similar to the intrinsic reward in CCFDM [Nguyen *et al.*, 2021], but the proposed CCLF does not require a forward dynamic model or action embedding that increases the model complexity.

5 Experiments and Results

5.1 Experimental Setup

We empirically evaluate the proposed CCLF in terms of sample efficiency and ultimate performance, on 6 continuous control tasks from the DMC suite [Tunyasuvunakool *et al.*, 2020], 26 discrete control tasks from the Atari Games [Bellemare *et al.*, 2013] and 3 navigation tasks with sparse extrinsic rewards from the MiniGrid [Chevalier-Boisvert *et al.*, 2018]. In this section, we mainly present the experimental results in the DMC suite with SAC being the base algorithm while detailed settings and results in the Atari Games and the MiniGrid are included in Appendix B.2, B.3, C.2, and C.3. For a comprehensive evaluation in the DMC suite, we include the following baselines to compare against:

- Pixel-based SAC (SAC-Pixel) [Haarnoja *et al.*, 2018]
- CURL [Laskin *et al.*, 2020a].
- DrQ [Yarats *et al.*, 2020] with $[K, M] = [2, 2]$ and a modified augmentation method for consistency.

- Hybrids of CURL and DrQ: CURL+ and CURL++, where contrastive representation learning is integrated to DrQ for $[K, M] = [2, 2]$ and $[5, 5]$ respectively.
- Augmented input selection models: 2 out of 5 inputs for each sample are selected by pixel overlap (Select) via Eq. (4) and contrastive curiosity (Select+) via Eq. (5) without the other curiosity-based components.

The detailed setting of hyper-parameters is provided in Appendix B.1. For our proposed CCLF, we initialize it with $[K, M] = [5, 5]$ to generate a sufficiently large amount of augmented inputs. For simplicity, we fix i^* randomly and only select j^* via Eq. (5) for the augmented input selection.

5.2 Results and Discussion

Not all Samples are Equally Important. In CURL+, data augmentation is applied twice for each sampled transition while 5 times in CURL++. Since CURL++ injects $2.5\times$ larger amount of inputs than CURL+, its computational complexity increases dramatically. Table 1 shows that CURL++ performs worse than CURL+ in 4 tasks at 100K steps and slightly outperforms CURL+ in only 2 tasks at 500K steps. In Figure 2 and Appendix Figure 5, the learning curve of CURL++ is clearly below CURL+ at first and gradually approaches to the same level as CURL+. Since more augmented inputs may not guarantee the consistency of semantics, additional training is often required for convergence. Therefore, we can empirically validate the hypothesis that not all augmented inputs are equally important and simply increasing the number of augmentations is instead inefficient. A similar result can be found DrQ Appendix F [Yarats *et al.*, 2020].

Main Results on the DMC Suite

The average sample efficiency and asymptotic performance are shown in Table 1 at 100K and 500K environment steps, respectively. Meanwhile, Figure 2 demonstrates the agent’s learning capability over 500K steps. Compared SAC-Pixel to the other models in Figure 2, its performance is not improved in all 6 tasks even until 500K steps while the other models can asymptotically perform well. Thus, it is challenging for the conventional SAC to learn directly from raw pixels and a sample-efficient RL method is needed to aid that.

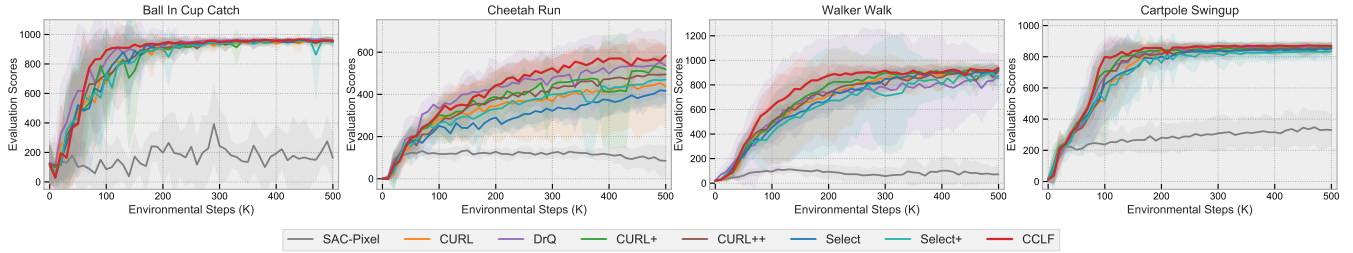


Figure 2: Learning performances on the continuous control tasks from the DMC Suite (Selected). The proposed CCLF on SAC outperforms the other baseline methods in terms of sample efficiency and converges much faster, averaged by 6 random runs.

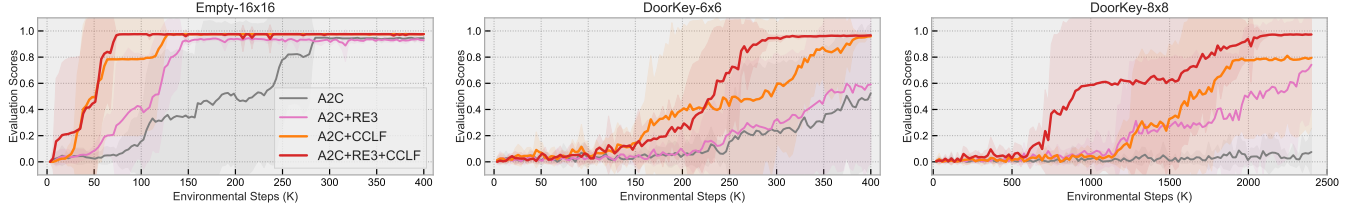


Figure 3: Learning performances on the navigation tasks from the MiniGrid. The proposed CCLF can be applied to both A2C and A2C+RE3. It significantly outperforms the other baselines in terms of sample efficiency and converges much faster, averaged by 5 random runs.

According to Table 1, Select performs better than Select+, on 3 tasks at 100K and 4 tasks at 500K, with more stable learning curves as shown in Figure 2. Indeed, the inputs in Select may contain some invariances to improve sample efficiency and learning capability. However, more under-learned inputs with even richer invariances are present in Select+, and agents cannot adapt the learning process in this model, causing the instability issue in Select+.

To tackle this issue, the proposed CCLF collaboratively adapts the learning process with the selected inputs and contrastive curiosity, so the learning curves become more smooth than others in Figure 2. In particular, CCLF outperforms all baselines in 5 tasks at both 100K and 500K regimes in Table 1. Moreover, it converges much faster than Select+ according to the results at 100K steps. In fact, the proposed CCLF only requires about 50% environment steps to converge to desirable performances on 3 tasks (Ball in Cup, Walker, and Cartpole) as the other baselines. In addition, it even benchmarks on Cheetah-Run and Finger-Spin tasks at 500K steps. Therefore, we can conclude that our proposed CCLF can improve the sample efficiency and learning capabilities of RL agents, with fewer environment interactions and 60% reduced augmented inputs. We also analyze the computational complexity on the Cartpole task by model sizes and training time in Appendix C.1, where CCLF can avoid increasing the training cost dramatically.

Additional Experiments in Atari Games. In addition to continuous control tasks, CCLF can also be incorporated into Rainbow DQN [Hessel *et al.*, 2018] to perform discrete control tasks. As shown in Appendix C.2, the proposed CCLF attains state-of-the-art performances in 8 out of 26 Atari Games at 100K steps. In particular, CCLF is superior to CURL in 11 games and DrQ in 18 games, which favorably indicates the effectiveness of improving sample efficiency.

Further Investigation on MiniGrid. Apart from off-policy algorithms, we also investigate the compatibility on the on-policy algorithm. More specifically, we apply the proposed CCLF to A2C [Mnih *et al.*, 2016] and RE3 [Seo *et al.*, 2021]

to perform navigation tasks with sparse rewards in MiniGrid. We first adapt CCLF to the on-policy algorithm by removing the experience replay component. Note that the input from MiniGrid is already a compact and efficient $7 \times 7 \times 3$ embedding of partially-observable 7×7 grids, so even slight augmentation will induce highly inconsistent learned features. Thus, we directly duplicate the embedding without random augmentations to obtain contrastive curiosity for regularization and intrinsic reward. Figure 3 shows that CCLF exhibits superior sample efficiency and learning capabilities in all three tasks, even model-agnostic with the state-of-the-art curiosity-driven method RE3. In the Empty-16 \times 16 task, our CCLF can reach the optimal level in about 50% and 55% of the training steps of RE3 and A2C, respectively. By comparing the ultimate performance scores, the proposed CCLF obtains $1.63\times$ higher average performance than RE3 in DoorKey-6 \times 6 and $1.3\times$ in DoorKey-8 \times 8.

Effectiveness of the Proposed RL Components. One might wonder if the proposed CCLF benefits mainly from one or several curiosity-based components in practice. Hence, we empirically examine the effectiveness of all possible combinations of the four curiosity-driven components on the Cartpole task from the DMC suite. The results are included in Appendix C.4, where it can be concluded that all four components are necessary and important to attain state-of-the-art performances. Our proposed CCLF can navigate all four RL components together to improve the sample efficiency and resolve instability, which demonstrates effective collaboration.

6 Conclusion

In this paper, we present CCLF, a contrastive-curiosity-driven learning framework for RL with visual observations, which can significantly improve the sample efficiency and learning capabilities of agents. As we empirically find that not all samples nor their augmented inputs are equally important for RL, CCLF encourages agents to learn in a curious way, exploiting sample complexity and importance systemically.

References

- [Aubret *et al.*, 2019] Arthur Aubret, Laetitia Matignon, and Salima Hassas. A survey on intrinsic motivation in reinforcement learning. *arXiv:1908.06976*, 2019.
- [Bellemare *et al.*, 2013] Marc G Bellemare, Yavar Naddaf, Joel Veness, and Michael Bowling. The arcade learning environment: An evaluation platform for general agents. *JAIR*, 47, 2013.
- [Bellemare *et al.*, 2016] Marc Bellemare, Sriram Srinivasan, Georg Ostrovski, Tom Schaul, David Saxton, and Remi Munos. Unifying count-based exploration and intrinsic motivation. *NeurIPS*, 29:1471–1479, 2016.
- [Berlyne, 1960] Daniel E Berlyne. Conflict, arousal, and curiosity. 1960.
- [Burda *et al.*, 2018] Yuri Burda, Harrison Edwards, Amos Storkey, and Oleg Klimov. Exploration by random network distillation. *arXiv preprint arXiv:1810.12894*, 2018.
- [Chevalier-Boisvert *et al.*, 2018] Maxime Chevalier-Boisvert, Lucas Willems, and Suman Pal. Minimalistic gridworld environment for openai gym. <https://github.com/maximecb/gym-minigrid>, 2018.
- [Cobbe *et al.*, 2019] Karl Cobbe, Oleg Klimov, Chris Hesse, Taehoon Kim, and John Schulman. Quantifying generalization in reinforcement learning. In *ICML*, pages 1282–1289. PMLR, 2019.
- [Fortunato *et al.*, 2017] Meire Fortunato, Mohammad Gheshlaghi Azar, Bilal Piot, Jacob Menick, Ian Osband, Alex Graves, Vlad Mnih, Remi Munos, Demis Hassabis, Olivier Pietquin, et al. Noisy networks for exploration. *arXiv preprint arXiv:1706.10295*, 2017.
- [Haarnoja *et al.*, 2018] Tuomas Haarnoja, Aurick Zhou, Kristian Hartikainen, George Tucker, Sehoon Ha, Jie Tan, Vikash Kumar, Henry Zhu, Abhishek Gupta, Pieter Abbeel, et al. Soft actor-critic algorithms and applications. *arXiv preprint arXiv:1812.05905*, 2018.
- [Hafner *et al.*, 2019a] Danijar Hafner, Timothy Lillicrap, Jimmy Ba, and Mohammad Norouzi. Dream to control: Learning behaviors by latent imagination. In *International Conference on Learning Representations*, 2019.
- [Hafner *et al.*, 2019b] Danijar Hafner, Timothy Lillicrap, Ian Fischer, Ruben Villegas, David Ha, Honglak Lee, and James Davidson. Learning latent dynamics for planning from pixels. In *ICML*, pages 2555–2565. PMLR, 2019.
- [He *et al.*, 2020] Kaiming He, Haoqi Fan, Yuxin Wu, Saining Xie, and Ross Girshick. Momentum contrast for unsupervised visual representation learning. In *Proceedings of the IEEE/CVF Conference on Computer Vision and Pattern Recognition*, pages 9729–9738, 2020.
- [Hessel *et al.*, 2018] Matteo Hessel, Joseph Modayil, Hado Van Hasselt, Tom Schaul, Georg Ostrovski, Will Dabney, Dan Horgan, Bilal Piot, Mohammad Azar, and David Silver. Rainbow: Combining improvements in deep reinforcement learning. In *AAAI*, 2018.
- [Kaiser *et al.*, 2019] Lukasz Kaiser, Mohammad Babaeizadeh, Piotr Milos, Blazej Osinski, Roy H Campbell, Konrad Czechowski, Dumitru Erhan, Chelsea Finn, Piotr Kozakowski, Sergey Levine, et al. Model-based reinforcement learning for atari. *arXiv preprint arXiv:1903.00374*, 2019.
- [Kielak, 2019] Kacper Piotr Kielak. Do recent advancements in model-based deep reinforcement learning really improve data efficiency? 2019.
- [Kingma and Ba, 2014] Diederik P Kingma and Jimmy Ba. Adam: A method for stochastic optimization. *arXiv preprint arXiv:1412.6980*, 2014.
- [Laskin *et al.*, 2020a] Michael Laskin, Aravind Srinivas, and Pieter Abbeel. Curl: Contrastive unsupervised representations for reinforcement learning. In *ICML*, pages 5639–5650. PMLR, 2020.
- [Laskin *et al.*, 2020b] Misha Laskin, K. Lee, A. Stooke, L. Pinto, Pieter Abbeel, and Aravind Srinivas. Reinforcement learning with augmented data. *NeurIPS*, 33, 2020.
- [Lee *et al.*, 2019] Alex X Lee, Anusha Nagabandi, Pieter Abbeel, and Sergey Levine. Stochastic latent actor-critic: Deep reinforcement learning with a latent variable model. *arXiv preprint arXiv:1907.00953*, 2019.
- [LEE *et al.*, 2020] KIMIN LEE, Kibok Lee, Jinwoo Shin, and Honglak Lee. Network randomization: A simple technique for generalization in deep reinforcement learning. In *Eighth International Conference on Learning Representations, ICLR 2020. International Conference on Learning Representations*, 2020.
- [Lei Ba *et al.*, 2016] Jimmy Lei Ba, Jamie Ryan Kiros, and Geoffrey E Hinton. Layer normalization. *ArXiv e-prints*, pages arXiv–1607, 2016.
- [Li *et al.*, 2021] Kevin Li, Abhishek Gupta, Ashwin Reddy, Vitchyr H Pong, Aurick Zhou, Justin Yu, and Sergey Levine. Mural: Meta-learning uncertainty-aware rewards for outcome-driven reinforcement learning. In *ICML*. PMLR, 2021.
- [Lin *et al.*, 2019] Yijiong Lin, Jiancong Huang, Matthieu Zimmer, Juan Rojas, and Paul Weng. Towards more sample efficiency in reinforcement learning with data augmentation. *arXiv preprint arXiv:1910.09959*, 2019.
- [Liquin and Lombrozo, 2020] Emily G Liquin and Tania Lombrozo. Explanation-seeking curiosity in childhood. *Current Opinion in Behavioral Sciences*, 35:14–20, 2020.
- [Malik *et al.*, 2021] Dhruv Malik, Aldo Pacchiano, Vishwak Srinivasan, and Yuanzhi Li. Sample efficient reinforcement learning in continuous state spaces: A perspective beyond linearity. In *ICML*. PMLR, 2021.
- [Mnih *et al.*, 2013] Volodymyr Mnih, Koray Kavukcuoglu, David Silver, Alex Graves, Ioannis Antonoglou, Daan Wierstra, and Martin Riedmiller. Playing atari with deep reinforcement learning. *arXiv preprint arXiv:1312.5602*, 2013.
- [Mnih *et al.*, 2015] Volodymyr Mnih, Koray Kavukcuoglu, David Silver, Andrei A Rusu, Joel Veness, Marc G Bellemare, Alex Graves, Martin Riedmiller, Andreas K Fidjeland, Georg Ostrovski, et al. Human-level control through deep reinforcement learning. *nature*, 518(7540):529–533, 2015.
- [Mnih *et al.*, 2016] Volodymyr Mnih, Adria Puigdomenech Badia, Mehdi Mirza, Alex Graves, Timothy Lillicrap, Tim Harley, David Silver, and Koray Kavukcuoglu. Asynchronous methods for deep reinforcement learning. In *ICML*. PMLR, 2016.
- [Nguyen *et al.*, 2021] Thanh Nguyen, Tung M Luu, Thang Vu, and Chang D Yoo. Sample-efficient reinforcement learning representation learning with curiosity contrastive forward dynamics model. *arXiv preprint arXiv:2103.08255*, 2021.
- [Oord *et al.*, 2018] Aaron van den Oord, Yazhe Li, and Oriol Vinyals. Representation learning with contrastive predictive coding. *arXiv preprint arXiv:1807.03748*, 2018.
- [Paszke *et al.*, 2019] Adam Paszke, Sam Gross, Francisco Massa, Adam Lerer, James Bradbury, Gregory Chanan, Trevor Killeen, Zeming Lin, Natalia Gimelshein, Luca Antiga, et al. Pytorch:

- An imperative style, high-performance deep learning library. *Advances in neural information processing systems*, 32:8026–8037, 2019.
- [Pathak *et al.*, 2017] Deepak Pathak, Pulkit Agrawal, Alexei A Efros, and Trevor Darrell. Curiosity-driven exploration by self-supervised prediction. In *ICML*, pages 2778–2787. PMLR, 2017.
- [Raileanu *et al.*, 2020] Roberta Raileanu, Max Goldstein, Denis Yarats, Ilya Kostrikov, and Rob Fergus. Automatic data augmentation for generalization in deep reinforcement learning. *arXiv preprint arXiv:2006.12862*, 2020.
- [Rakelly *et al.*, 2019] Kate Rakelly, Aurick Zhou, Chelsea Finn, Sergey Levine, and Deirdre Quillen. Efficient off-policy meta-reinforcement learning via probabilistic context variables. In *ICML*, pages 5331–5340. PMLR, 2019.
- [Saxe *et al.*, 2013] Andrew M Saxe, James L McClelland, and Surya Ganguli. Exact solutions to the nonlinear dynamics of learning in deep linear neural networks. *arXiv preprint arXiv:1312.6120*, 2013.
- [Schaul *et al.*, 2015] Tom Schaul, John Quan, Ioannis Antonoglou, and David Silver. Prioritized experience replay. *arXiv preprint arXiv:1511.05952*, 2015.
- [Schaul *et al.*, 2016] Tom Schaul, John Quan, Ioannis Antonoglou, and David Silver. Prioritized experience replay. In *ICLR*, 2016.
- [Schwarzer *et al.*, 2020] Max Schwarzer, Ankesh Anand, Rishabh Goel, R Devon Hjelm, Aaron Courville, and Philip Bachman. Data-efficient reinforcement learning with self-predictive representations. In *ICLR*, 2020.
- [Seo *et al.*, 2021] Younggyo Seo, Lili Chen, Jinwoo Shin, Honglak Lee, Pieter Abbeel, and Kimin Lee. State entropy maximization with random encoders for efficient exploration. *arXiv preprint arXiv:2102.09430*, 2021.
- [Spielberger and Starr, 2012] Charles D Spielberger and Laura M Starr. Curiosity and exploratory behavior. In *Motivation: Theory and research*, pages 231–254. 2012.
- [Sun *et al.*, 2022] Chenyu Sun, Hangwei Qian, and Chunyan Miao. From psychological curiosity to artificial curiosity: Curiosity-driven learning in artificial intelligence tasks. *arXiv preprint arXiv:2201.08300*, 2022.
- [Sutton and Barto, 1998] Richard S Sutton and Andrew G Barto. Reinforcement learning: an introduction mit press. *Cambridge, MA*, 22447, 1998.
- [Tieleman *et al.*, 2012] Tijmen Tieleman, Geoffrey Hinton, et al. Lecture 6.5-rmsprop: Divide the gradient by a running average of its recent magnitude. *COURSERA: Neural networks for machine learning*, 4(2):26–31, 2012.
- [Todorov *et al.*, 2012] Emanuel Todorov, Tom Erez, and Yuval Tassa. Mujoco: A physics engine for model-based control. In *2012 IEEE/RSJ International Conference on Intelligent Robots and Systems*, pages 5026–5033. IEEE, 2012.
- [Tunyasuvunakool *et al.*, 2020] Saran Tunyasuvunakool, Alistair Muldal, Yotam Doron, Siqi Liu, Steven Bohez, Josh Merel, Tom Erez, Timothy Lillicrap, Nicolas Heess, and Yuval Tassa. dm.control: Software and tasks for continuous control. *Software Impacts*, 6:100022, 2020.
- [Van Hasselt *et al.*, 2016] Hado Van Hasselt, Arthur Guez, and David Silver. Deep reinforcement learning with double q-learning. In *Proceedings of the AAAI conference on artificial intelligence*, volume 30, 2016.
- [van Hasselt *et al.*, 2019] Hado P van Hasselt, Matteo Hessel, and John Aslanides. When to use parametric models in reinforcement learning? *NeurIPS*, 32:14322–14333, 2019.
- [Wang *et al.*, 2016] Ziyu Wang, Tom Schaul, Matteo Hessel, Hado Hasselt, Marc Lanctot, and Nando Freitas. Dueling network architectures for deep reinforcement learning. In *International conference on machine learning*, pages 1995–2003. PMLR, 2016.
- [Wang *et al.*, 2020] Kaixin Wang, Bingyi K, Jie S, and Jiashi F. Improving generalization in reinforcement learning with mixture regularization. In *NeurIPS*, 2020.
- [Wu and Miao, 2013] Qiong Wu and Chunyan Miao. Curiosity: From psychology to computation. *ACM Computing Surveys (CSUR)*, 46(2):1–26, 2013.
- [Yarats *et al.*, 2020] Denis Yarats, Ilya Kostrikov, and Rob Fergus. Image augmentation is all you need: Regularizing deep reinforcement learning from pixels. In *ICLR*, 2020.
- [Yarats *et al.*, 2021a] Denis Yarats, Rob Fergus, Alessandro Lazaric, and Lerrel Pinto. Mastering visual continuous control: Improved data-augmented reinforcement learning. *arXiv preprint arXiv:2107.09645*, 2021.
- [Yarats *et al.*, 2021b] Denis Yarats, Amy Zhang, Ilya Kostrikov, Brandon Amos, Joelle Pineau, and Rob Fergus. Improving sample efficiency in model-free reinforcement learning from images. In *AAAI*, 2021.
- [Zhao and Tresp, 2019] Rui Zhao and Volker Tresp. Curiosity-driven experience prioritization via density estimation. *arXiv preprint arXiv:1902.08039*, 2019.

Appendix A Extended Background

A.1 Efficiency of Data Augmentation in RL

Data augmentation such as translation, crop, rotation, and cutout has been widely applied in computer vision but is only recently introduced in RL to incorporate invariances for representation learning [Cobbe *et al.*, 2019; Lin *et al.*, 2019; Raileanu *et al.*, 2020; LEE *et al.*, 2020; Laskin *et al.*, 2020b; Yarats *et al.*, 2020; Laskin *et al.*, 2020a]. In particular, RAD [Laskin *et al.*, 2020b] investigates several commonly used data augmentation methods, where random crop and translation are found most effective. Meanwhile, DrQ [Yarats *et al.*, 2020] regularizes the Q-function to ensure that multiple augmentations from the same observation should have similar Q-values. CURL [Laskin *et al.*, 2020a] leverages contrastive learning with data augmentation such that representation learning becomes more robust. When learning directly from raw pixels, these works have outperformed other methods, including pixel SAC [Haarnoja *et al.*, 2018], PlaNet [Hafner *et al.*, 2019b], Dreamer [Hafner *et al.*, 2019a], SLAC [Lee *et al.*, 2019] and SAC+AE [Yarats *et al.*, 2021b]. However, sample importance has not been fully exploited in any data augmentation based RL.

A.2 Soft Actor-Critic (SAC)

We consider a Markov Decision Process (MDP) setting with the state $s_t \in \mathcal{S}$, the action $a_t \in \mathcal{A}$, the transition probability P mapping from the current state s_t and action a_t to the next state s'_t , and the (extrinsic) reward $r_t^e \in \mathcal{R}$. SAC [Haarnoja *et al.*, 2018] is an off-policy model-free reinforcement learning (RL) algorithm that learns a stochastic policy π_ψ (actor) with state-action value functions Q_{ϕ_1}, Q_{ϕ_2} (critics), and a temperature coefficient α by encouraging exploration through a γ -discounted maximum-policy-entropy term. However, agents are often required to learn directly from high-dimensional visual observations $o_t \in \mathcal{O}$ rather than states s_t in practice.

In particular, the critics are trained by minimizing the squared Bellman error via uniformly sampling transitions $\tau_t = (o_t, a_t, r_t^e, d_t, o'_t)$ from a replay buffer \mathcal{B} ,

$$\mathcal{L}_Q(\phi) = \mathbb{E}_{\tau \sim \mathcal{B}} \left[(Q_\phi(o_t, a_t) - (r_t^e + \gamma(1 - d_t)\mathcal{T}_t))^2 \right]$$

where d_t is the done signal and the soft target value \mathcal{T}_t is implicitly parameterized as

$$\mathcal{T}_t = \min_{i=1,2} Q_{\bar{\phi}_i}(o'_t, a') - \alpha \log \pi_\psi(a'|o'_t).$$

$Q_{\bar{\phi}_i}$ is the exponential moving average (EMA) of Q_{ϕ_i} to impose training stability, and a' is sampled stochastically by the actor network using the next observation o'_t .

The actor network $\pi_\psi(a|o)$ is a parametric tanh-Gaussian which stochastically samples $a = \tanh(\mu_\psi(o) + \sigma_\psi(o)\epsilon)$ given the observation o , where $\epsilon \sim \mathcal{N}(0, 1)$, and μ_ψ and σ_ψ are the parametric mean and standard deviation, respectively. Meanwhile, the actor network is trained by minimizing the divergence from the exponential of the soft-Q function, equivalent to

$$\mathcal{L}_\pi(\psi) = -\mathbb{E}_{a \sim \pi} \left[\min_{i=1,2} Q_{\bar{\phi}_i}(o_t, a) - \alpha \log \pi_\psi(a|o_t) \right].$$

Finally, α controls the priority of entropy maximization and is optimized against a target entropy as

$$\mathcal{L}(\alpha) = \mathbb{E}_{a \sim \pi} [-\alpha \log \pi_\psi(a|o_t) - \alpha \bar{\mathcal{H}}]$$

where $\bar{\mathcal{H}} \in \mathbb{R}$ represents the target entropy with $\bar{\mathcal{H}} = -|\mathcal{A}|$.

A.3 Rainbow DQN

Rainbow DQN [Hessel *et al.*, 2018] is an off-policy deep RL algorithm for discrete action space, extending the conventional DQN [Mnih *et al.*, 2015] with multiple improvements of other DQN methods into a single learner. In particular, it utilizes the Double Q-Learning method [Van Hasselt *et al.*, 2016] to resolve overestimation bias. As an off-policy algorithm, it employs the Prioritized Experience Replay technique [Schaul *et al.*, 2015] to sample the novel transitions with high TD-errors more frequently. In addition, the dueling critic architecture network [Wang *et al.*, 2016] is incorporated to learn valuable states, avoiding determining the effect of all actions and states. Instead of the expected return, it uses distributional reinforcement learning to output a distribution over possible value function bins, with n -step learning [Sutton and Barto, 1998] and noisy linear layers [Fortunato *et al.*, 2017] for better exploration. Combining all above-mentioned techniques and architectures, Rainbow DQN can obtain state-of-the-art sample efficiency on Atari Games [Bellemare *et al.*, 2013] benchmarks. To further enhance the sample efficiency, an optimized configuration of Rainbow DQN hyperparameters is proposed to benchmark Atari Games at 100K training steps [van Hasselt *et al.*, 2019].

A.4 Advantage Actor-Critic (A2C)

In contrast to SAC and Rainbow DQN from off-policy RL algorithms, Advantage Actor Critic (A2C) [Mnih *et al.*, 2016] is an on-policy algorithm that combines the policy-based method (an actor) and value-based method (a critic), with an advantage function. While the value function measures how good the agent is at each state, the advantage function $A(s, a)$ captures how better an action a against the others at a given state s ,

$$A(s, a) = Q(s, a) - V(s).$$

Subsequently, the actor can leverage this information to optimize the agent's policy. As the result, the high variance of policy gradient can be greatly reduced to stabilize the model. Based on A2C, RE3 [Seo *et al.*, 2021] proposed to incorporate the state entropy as an intrinsic reward to encourage efficient exploration, which can be estimated with a fixed random encoder. RE3 has been shown to be capable of improving the sample efficiency on navigation tasks from the MiniGrid [Chevalier-Boisvert *et al.*, 2018] benchmark.

A.5 Contrastive Unsupervised RL (CURL)

To learn a meaningful representation from raw pixels, CURL [Laskin *et al.*, 2020a] utilizes data augmentation and contrastive learning to train an image encoder $f_\theta(o)$ in a self-supervised way, imposing an instance discrimination between similar and dissimilar encoded states. Given a batch of visual observations o , each is augmented twice and encoded into a query $q = f_\theta(o_q)$ and a key $k = f_{\bar{\theta}}(o_k)$, where the positive

keys k^+ indicate that both o_k and o_q are augmented from the same o and otherwise negative keys k^- . The key encoder $f_{\bar{\theta}}$ is a momentum-based moving average [He *et al.*, 2020] of the query encoder f_{θ} to ensure consistency and stability, where f_{θ} is learned by enforcing q to match with k^+ and keep far apart from k^- . The contrastive loss term to optimize the query encoder is defined as

$$\mathcal{L}_f(\theta) = - \sum_{b=1}^B \log \frac{\text{sim}(q_b, k^+)}{\text{sim}(q_b, k^+) + \sum_{l=1}^{B-1} \text{sim}(q_b, k_l^-)}$$

where B is the batch size and $\text{sim}(q, k) = q^T W k$ is the bi-linear inner-product to measure the similarity between q and k [Oord *et al.*, 2018].

Appendix B Experimental Settings

We conduct experiments on four cloud servers and one physical server with the following configurations.

- Operation System: Ubuntu 18.04
- Memory: 32GiB / 32GiB / 32GiB / 32GiB / 128GiB
- CPU: Intel Core Processor (Skylake) / Intel Core Processor (Skylake) / Intel Core Processor (Skylake) / Intel(R) Xeon(R) CPU E5-2620 v2 @ 2.10GHz
- vCPU: 8 / 8 / 16 / 16 / 24
- GPU: 2 \times NVIDIA Tesla P100 16GB / 2 \times NVIDIA Tesla P100 16GB / 1 \times NVIDIA Tesla V100S PCIE 32GB / 1 \times NVIDIA Tesla V100S PCIE 32GB / 2 \times NVIDIA GeForce RTX 3090 24GB

Our proposed CCLF is implemented using PyTorch [Paszke *et al.*, 2019] based on CURL [Laskin *et al.*, 2020a], where the contrastive learning module is incorporated to jointly improve the representation learning and Q-learning. As CCLF is model-agnostic, it can be applied to different base RL algorithms with some adaptations. In this paper, we mainly focus on SAC [Haarnoja *et al.*, 2018] as the base algorithm while additional experiments with Rainbow DQN [Hessel *et al.*, 2018] and A2C [Mnih *et al.*, 2016] have also been carried out on a diverse range of exploration tasks from Atari Games [Bellemare *et al.*, 2013] and MiniGrid [Chevalier-Boisvert *et al.*, 2018]. The implementation details are as follows.

B.1 Implementation of CCLF on SAC for Continuous Control Tasks in DMC Suite

Encoder Network

We utilize the same encoder network as SAC-AE [Yarats *et al.*, 2021b]. In particular, it is parameterized as 4 convolution layers with the ReLU activation, 3×3 kernels, and 32 channels. The stride is set to be 2 for the first layer and is reduced to 1 thereafter. Subsequently, the output is passed to a single normalized fully-connected layer by LayerNorm [Lei Ba *et al.*, 2016] with the tanh nonlinearity applied at the end. Finally, the orthogonal initialization [Saxe *et al.*, 2013] is performed to initialize the parameters for all convolutional layers as well as the fully-connected linear layer, where the bias is set to be zero.

Actor and Critic Networks

Both the actor and critic networks employ the image encoder network as described above to encode pixel observations, and their convolution layers share the same weights. During batch learning, these weights can only be updated by the critic optimizer and the contrastive optimizer. In other words, we detach the actor encoder to stop the propagation of the shared convolution layers during the actor update.

For the actor network, the encoded state representation is fed into a 3-layer MLP with the ReLU activation to output the policy mean and covariance for the diagonal Gaussian. Similarly, the critic networks pass the encoded state representation into a 3-layer MLP with the ReLU activation after each layer except for the last one. For both actor and critic networks, we set the hidden dimension to 1024.

It should be noted that the clipped double Q-learning [Van Hasselt *et al.*, 2016] is utilized for critic networks, a popular technique for stability in SAC-based methods. Meanwhile, the target critic network is momentum-based updated by the critic network to impose Q-learning stability. When we train the critics, only the parameters of the critic networks are updated by the optimizer.

Contrastive Learning

Following the same implementation of CURL [Laskin *et al.*, 2020a], the contrastive learning module is built with the image encoder networks in the critics. In particular, the query is encoded by the encoder in the critic network and the keys are encoded by the encoder in the target network. The key encoder is also momentum-based updated by the query encoder to avoid instability [He *et al.*, 2020]. To measure the similarity between query and keys, the bi-linear inner-product is utilized and its weight is initialized randomly.

Training and Evaluation Setup

During the model training, the 100×100 visual observations are randomly cropped to 84×84 pixels. We first collect 1000 transitions using a random policy and store them in the replay buffer. After that, the subsequent transition tuples are collected by sampling actions from the current policy. Meanwhile, the model update is performed by sampling a mini-batch of transition tuples from the replay buffer at each training step. For clarification, the environment step in this section refers to the multiplication of action repeat and training steps. For example, 50K training steps with the action repeat of 2 represents 100K environment steps. For a fair evaluation, all models are trained with 6 random seeds, during which agents are evaluated every 10K environment steps with 10 episodes. During the evaluation, the 100×100 visual observations are center cropped to 84×84 pixels and agents perform with the deterministic policy outputted by the actor network instead of sampling a stochastic action.

Environments

We evaluate the proposed CCLF from the perspectives of both sample efficiency and ultimate performance on six continuous control tasks in the DMC suite [Tunyasuvunakool *et al.*, 2020]. The DMC suite provides a diverse collection of complex control using MuJoCo physics [Todorov *et al.*,

2012] with different settings such as sparse rewards and complex dynamics, which are challenging for agents to operate directly from visual observations. The six tasks are commonly used as benchmarks to evaluate the agent’s performance, where the evaluation metric is the performance score in the range of [0, 1000].

Hyper-parameters

Throughout all experiments, the network hyper-parameters are kept fixed and consistent unless otherwise stated. We employ the Adam optimizer [Kingma and Ba, 2014] and set the batch size to 512. To capture both spatial and temporal information, 3 consecutive frames are stacked into one observation. The detailed setting of hyper-parameters for baseline models is listed in Table 2, which follows the same settings of CURL [Laskin *et al.*, 2020a] and DrQ [Yarats *et al.*, 2020].

Hyper-parameters	Value
Observation rendering	(100, 100)
Observation downsampling	(84, 84)
Replay buffer size	100K
Initial steps	1K
Stacked frames	3
Action repeat	2 Finger, Spin; Walker, walk 8 Cartpole, Swingup 4 otherwise
Hidden units (MLP)	1024
Evaluation episodes	10
Optimizer	Adam
$(\beta_1, \beta_2) \rightarrow (f_\theta, \pi_\psi, Q_\phi)$	(.9, .999)
$(\beta_1, \beta_2) \rightarrow \alpha$	(.5, .999)
Learning rate $(f_\theta, \pi_\psi, Q_\phi)$	$2e - 4$ cheetah, run $1e - 3$ otherwise
Learning rate	$1e - 4$
Batch Size	512
Initial temperature	0.1
Q function EMA rate	0.01
Critic target update frequency	2
Actor update frequency	2
Actor log stddev bounds	[-10, 2]
Convolutional layers	4
Number of filters	32
Activation	ReLU
Encoder EMA rate	0.05
Encoder feature dimension	50
Discount factor	0.99

Table 2: Hyper-parameters used for CURL and DrQ based models with SAC being the base algorithm. Most hyper-parameters are fixed for all tasks while only action repeat and learning rate vary across different tasks.

For the proposed CCLF, we initialize it with $[K, M] = [5, 5]$ to generate a sufficiently large amount of augmented inputs. In addition to the hyper-parameters set in Table 2, we list the other hyper-parameters used in CCLF in Table 3, which are fixed when evaluating on the six continuous control tasks in the DMC suite.

Hyper-parameters	Value
$[K, M]$	$[5, 5]$
Momentum coefficient for prioritization	0.99
Intrinsic reward decay weight	$2e - 5$
Intrinsic reward temperature	0.2

Table 3: Additional hyper-parameters used for the proposed CCLF on SAC, fixed across all evaluated tasks.

B.2 Implementation of CCLF on Rainbow DQN for Discrete Control Tasks in Atari Games

Following the similar setting and rationale in CURL, we are able to extend CCLF on discrete control tasks from Atari100K with minimal modifications. In particular, we select the Rainbow DQN with the data-efficient architecture (Efficient Rainbow) [van Hasselt *et al.*, 2019] as the base algorithm for our proposed model-agnostic CCLF. For the encoder network, actor and critic networks, and contrastive learning module, we follow the exactly same network architectures as CURL Rainbow, from the publicly available repository https://github.com/aravindsrinivas/curl_rainbow. To incorporate the curiosity-driven experienced replay component, we modify the algorithm by replacing the TD-error-based prioritization with our proposed contrastive-curiosity-based prioritization, where the sampling weights are updated in a momentum manner.

Training and Evaluation Setup

During the model training, the 84×84 visual observations are randomly cropped to 80×80 pixels, padded by 4 pixels and then randomly cropped again to 84×84 pixels. We first collect 1600 transitions using a random policy and store them in the replay buffer. After that, the subsequent transition tuples are collected using the outputted actions from the current policy. Meanwhile, the model update is performed by sampling a mini-batch of transition tuples from the replay buffer at each training step. For a fair evaluation, our CCLF is trained with 4 random seeds, during which agents are evaluated every 10K training steps with 10 episodes. During the evaluation, the 84×84 rendered observations are directly inputted into the trained model without further augmentations. We evaluate CCLF from the perspective of sample efficiency at 100K training steps on 26 discrete control tasks in the Atari Games.

Hyper-parameters

Throughout all experiments, the network hyper-parameters are kept fixed and consistent unless otherwise stated. For a fair comparison and evaluation, the same hyper-parameters used in CURL on the Rainbow DQN are also utilized in our experiments. To further stabilize the model training, we set a coefficient for the contrastive loss term, which is consistent with the CURL method. We employ the Adam optimizer [Kingma and Ba, 2014] and set the batch size to 32. To capture both spatial and temporal information, 4 consecutive frames are stacked into one observation. The detailed setting of hyper-parameters is provided in Table 4 and Table 5.

Hyperparameter	Value
Data augmentation	Random Crop
Grey-scaling	TRUE
Observation	(84, 84)
Frames stacked	4
Action repetitions	4
Replay buffer size	100K
Replay period	1
Min replay size for sampling	1600
Training steps	100K
Training frames	400K
Reward clipping	[-1,1]
Max frames per episode	108K
Minibatch size	32
Discount factor	0.99
Optimizer	Adam
Optimizer: learning rate	0.0001
Optimizer: β_1	0.9
Optimizer: β_2	0.999
Optimizer: ϵ	0.00015
Max gradient norm	10
Q network: channels	32, 64
Q network: filter size	$5 \times 5, 5 \times 5$
Q network: stride	5, 5
Q network: hidden units	256
Non-linearity	ReLU
Multi step return	20
Update	Distributional Double Q
Support-of-Q-distribution	51 bins
Dueling	TRUE
Target network update period	Every 2000 updates
Exploration	Noisy Nets
Noisy nets parameter 0.1	0.1
Momentum (EMA for key encoder update)	0.001

Table 4: Hyper-parameters used for CURL and DrQ based models with Rainbow DQN being the base algorithm.

Hyperparameter	Value
$[K, M]$	[5, 5]
Coefficient of contrastive loss term	1 for alien, bank heist, battle zone, kangaroo, kung fu master, and ms pacman; 0.0001 otherwise
Momentum coefficient for prioritization	0.99
Intrinsic reward decay weight	$2e-5$
Intrinsic reward temperature	$2e-4$

Table 5: Additional hyper-parameters used for CCLF on Rainbow DQN. Most hyper-parameters are fixed for all tasks while only the coefficient of contrastive loss term varies across different tasks.

B.3 Implementation of CCLF on A2C for Navigation Tasks in MiniGrid

In addition to the off-policy RL algorithms, we further demonstrate that CCLF can be applied to the on-policy RL algorithm A2C with minimal modifications. Note that A2C does not employ the replay buffer for experience replay, thus we remove the curiosity-based prioritization component. Moreover, we also apply our CCLF to RE3 that proposed another type of intrinsic reward to encourage entropy-based exploration in the base algorithm of A2C. In particular, for the encoder network as well as actor and critic networks, we utilize the publicly available implementation repository https://github.com/younggyoseo/RE3/tree/master/a2c_re3 with the default hyperparameters for the A2C implementation in MiniGrid benchmark. For the contrastive learning module, the query network is built with the encoder network shared by the actor and critic, while the key network is momentum-based updated from the query. To measure the similarity between query and keys, the bi-linear inner-product is utilized and its weight is initialized randomly.

Training and Evaluation Setup

Hyperparameter	Value
Input Size	(7, 7, 3)
Replay buffer size (for RE3 intrinsic reward)	10K
Stacked frames	1
Action repeat	1
Evaluation episodes	100
Optimizer	RMSprop
Number of processes	16
Frames per process	8
Discount	0.99
GAE λ	0.95
Entropy coefficient	0.001
Value loss term coefficient	0.5
Maximum norm of gradient	0.5
RMSprop ϵ	0.05
Clipping ϵ	0.2
Recurrence	None
Training Steps	400K for Empty-16x16 and DoorKey-6x6; 2400K for DoorKey-8x8
Evaluation frequency	3200 for Empty-16x16 and DoorKey-6x6; 19200 for DoorKey-8x8
RE3: intrinsic reward coefficient	0.1 in Empty-16x16; 0.005 in DoorKey-6x6; 0.001 in DoorKey-8x8
RE3: k	3

Table 6: Hyper-parameters used for baselines of A2C and RE3. Most hyper-parameters are fixed for all tasks while the training steps, evaluation frequency and RE3 intrinsic reward coefficient change across different tasks as specified in RE3 settings.

During the model training, the $7 \times 7 \times 3$ input from MiniGrid is directly passed to the base RL learner and contrastive

learning without augmentations or input selection. It is because any small augmentation on embedded values will cause highly inconsistent learned features. The on-policy agent first collects 8 frames of transitions per process with a total of 16 processes during one update. For a fair evaluation, our CCLF is trained with 5 random seeds and the mean scores are plotted to demonstrate the learning capabilities. We evaluate the proposed CCLF from the perspective of sample efficiency at 400K training steps on Empty-16×16 and DoorKey-6×6 while 2400K steps on DoorKey-8×8 in the MiniGrid, consistent with the baseline settings.

Hyper-parameters

In order to carefully examine the benefits of our CCLF without any other changes, we employ the exact same hyper-parameters specified in the RE3 paper appendix Section C [Seo *et al.*, 2021]. Throughout all experiments, the network hyper-parameters are kept fixed and consistent unless otherwise stated. To further stabilize the model training, we set a coefficient for the contrastive loss term. We employ the RM-Sprop optimizer [Tieleman *et al.*, 2012] and present a full list of hyperparameters that are used for baselines in Table 6 as well as CCLF in Table 7.

Hyperparameter	Value
Contrastive: hidden units	128
Non-linearity	ReLU
Momentum (EMA for key encoder update)	0.001
Coefficient for contrastive loss	0.0001
Intrinsic reward decay weight	2e-5
Intrinsic reward temperature	2e-4

Table 7: Additional hyper-parameters used for the proposed CCLF on A2C and RE3, fixed across different tasks.

Appendix C Experimental Results

C.1 Additional Results on the DMC Suite

Overall Performance

The full learning performances on all six continuous control tasks are shown in Figure 5, where the proposed CCLF enables the agent to outperform other baseline models in sample efficiency. To compare the overall performance of CCLF against the baselines, we average the performances over the 6 selected control tasks in the DMC suite. The results are shown in Figure 6, where CCLF significantly surpasses the other models at both 100K and 500K environment steps. At 100K environment steps, our CCLF achieves a $1.14 \times$ mean score of the second-best model (DrQ), indicating a significant improvement of the sample efficiency. At 500K environment steps, the average score of CCLF is $1.04 \times$ mean score of the second-best model (CURL+). In a nutshell, our proposed CCLF can obtain state-of-the-art performance from the perspectives of sample efficiency and learning capabilities.

Comparison of Computational Complexity

Model Sizes. Figure 7 shows the average model size across different models during training. As we employ five servers

with different configurations, we take the mean size of the models running on different servers. It can be observed from Figure 7 that when increasing the number of augmentation inputs $[K, M]$ for both DrQ and CURL+DrQ, their model sizes increase substantially, which cause the increase of computational complexity as well. However, CCLF only requires relatively small model sizes and can efficiently reduce the prohibitive cost. In particular, CCLF only selects the **two** most informative augmented inputs from the **five** augmented inputs $[K, M] = [5, 5]$ respectively for both current observations and next observations, where the amount of inputs is reduced by 60%. On the one hand, our CCLF reduces 33% and 34.5% of the model sizes, respectively, compared to DrQ [5, 5] and CURL+DrQ [5, 5]. On the other hand, CCLF only slightly increases the model size by 10.1% and 10.6% compared to DrQ [2, 2] and CURL+DrQ [2, 2], and does not exceed DrQ [3, 3] nor CURL+DrQ [3, 3]. Therefore, we can conclude that the proposed CCLF is capable of learning efficiently by avoiding increasing the model complexity during agent learning.

Training Time. To compare the computational complexity by model training time, we average on the Cartpole-Swingup task across 6 runs. Figure 4 shows the average training time required by different models. It can be observed that increasing the number of augmented inputs per sample will result in a significant increase (around 33%) of training time by comparing CURL+ (2 inputs) and CURL++ (5 inputs). However, CCLF can reduce about 50% of the increased time caused by CURL++. Overall, it only costs a moderate level of training time increase compared to both DrQ and CURL+. Therefore, we may conclude that our proposed CCLF does not require too much additional running time and can efficiently reduce the unnecessary computational cost by avoiding injecting too many inputs.

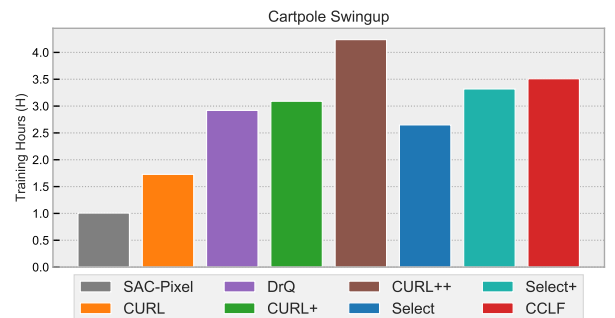


Figure 4: Average training hours on the Cartpole-Swingup task by different models.

C.2 Results on Atari Games

We present the results on Atari Games at 100K training steps in Table 8. Overall, the proposed CCLF achieves the state-of-the-art performance on 8 out of 26 games. In particular, we include the following baselines to compare against:

- Random Agent and Human Performance (Human).
- SimPLe [Kaiser *et al.*, 2019], a model-based algorithm.
- OverTrained Rainbow (OTRainbow) [Kielak, 2019].

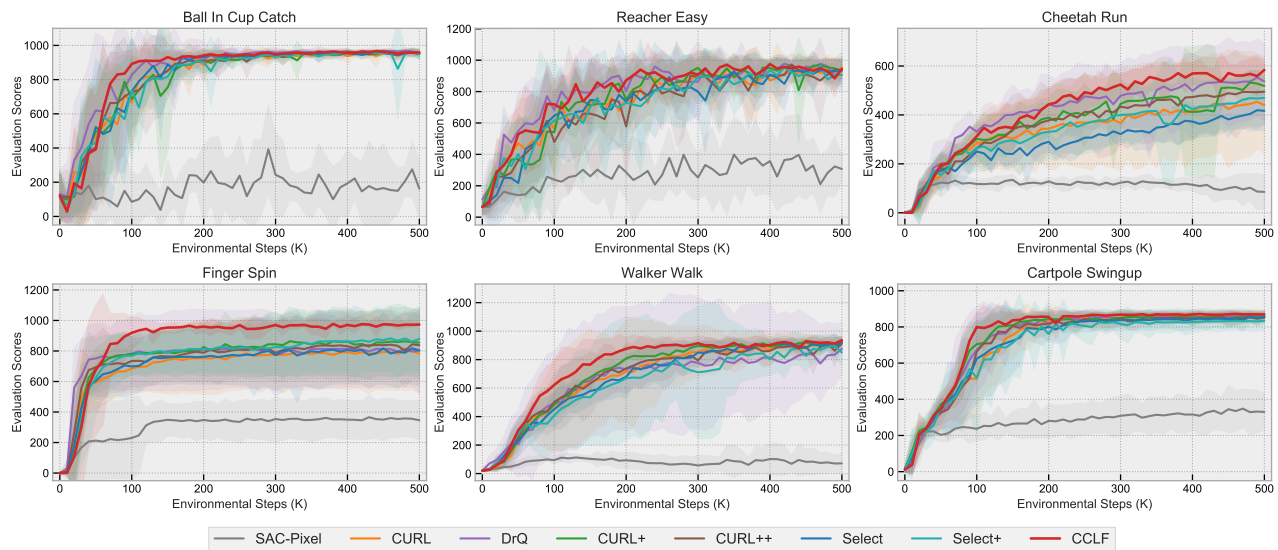


Figure 5: Comparison of the sample efficiency and learning performances against baselines on the 6 continuous control tasks from the DMC Suite. Our proposed CCLF outperforms the other methods in terms of sample efficiency and converges much faster than the baselines.

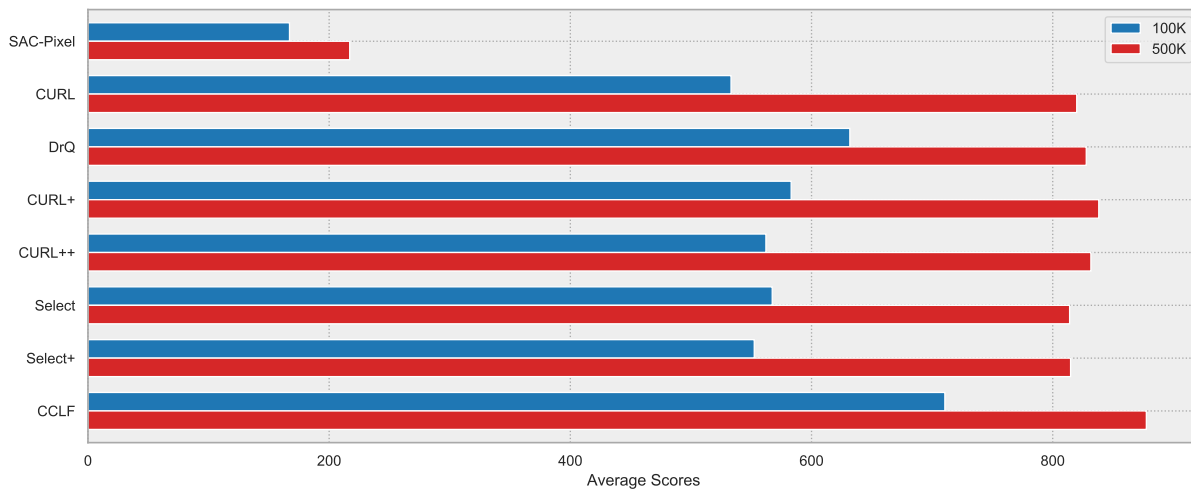


Figure 6: Comparison of average scores at 100K and 500K environment scores for DMC Suite

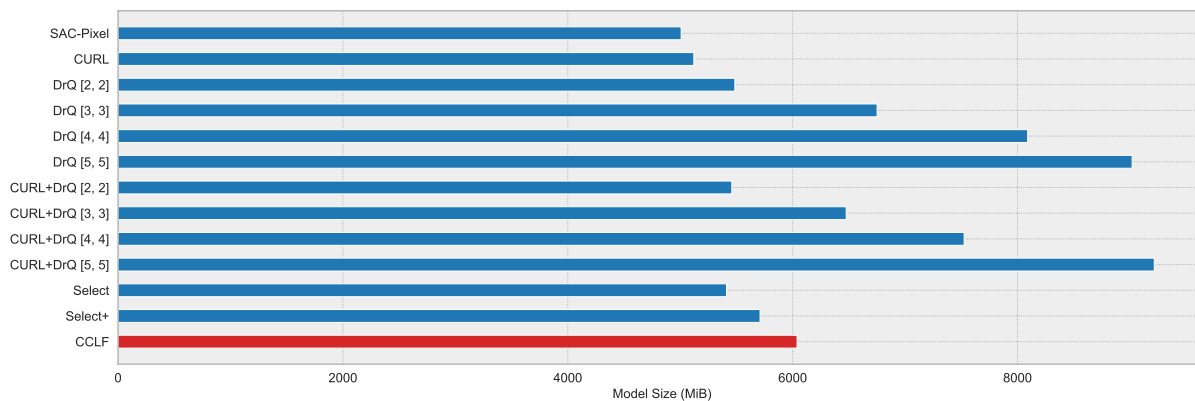


Figure 7: Comparison of model sizes during training

Atari100K Games	Human	Random	SimPLe	OTRainbow	Eff. Rainbow	Eff. DQN	CURL	DrQ	CCLF
ALIEN	7127.7	227.8	616.9	824.7	739.9	558.1	558.2	771.2	920.0
AMIDAR	1719.5	5.8	88.0	82.8	188.6	63.7	142.1	102.8	154.7
ASSAULT	742.0	222.4	527.2	351.9	431.2	589.5	600.6	452.4	612.4
ASTERIX	8503.3	210.0	1128.3	628.5	470.8	341.9	734.5	603.5	708.8
BANK HEIST	753.1	14.2	34.2	182.1	51.0	74.0	131.6	168.9	36.0
BATTLE ZONE	37187.5	2360.0	5184.4	4060.6	10124.6	4760.8	14870.0	12954.0	5775.0
BOXING	12.1	0.1	9.1	2.5	0.2	-1.8	1.2	6.0	7.4
BREAKOUT	30.5	1.7	16.4	9.8	1.9	7.3	4.9	16.1	2.7
CHOPPER COMMAND	7387.8	811.0	1246.9	1033.3	861.8	624.4	1058.5	780.3	765.0
CRAZY CLIMBER	35829.4	10780.5	62583.6	21327.8	16185.3	5430.6	12146.5	20516.5	7845.0
DEMON ATTACK	1971.0	152.1	208.1	711.8	508.0	403.5	817.6	1113.4	1360.9
FREEWAY	29.6	0.0	20.3	25.0	27.9	3.7	26.7	9.8	22.6
FROSTBITE	4334.7	65.2	254.7	231.6	866.8	202.9	1181.3	331.1	1401.0
GOPHER	2412.5	257.6	771.0	778.0	349.5	320.8	669.3	636.3	814.7
HERO	30826.4	1027.0	2656.6	6458.8	6857.0	2200.1	6279.3	3736.3	6944.5
JAMESBOND	302.8	29.0	125.3	112.3	301.6	133.2	471.0	236.0	308.8
KANGAROO	3035.0	52.0	323.1	605.4	779.3	448.6	872.5	940.6	650.0
KRULL	2665.5	1598.0	4539.9	3277.9	2851.5	2999.0	4228.6	4018.1	3975.0
KUNG FU MASTER	22736.3	258.5	17257.2	5722.2	14346.1	2020.9	14307.8	9111.0	12605.0
MS PACMAN	6951.6	307.3	1480.0	941.9	1204.1	872.0	1465.5	960.5	1397.5
PONG	14.6	-20.7	12.8	1.3	-19.3	-19.4	-16.5	-8.5	-17.3
PRIVATE EYE	69571.3	24.9	58.3	100.0	97.8	351.3	218.4	-13.6	100.0
QBERT	13455.0	163.9	1288.8	509.3	1152.9	627.5	1042.4	854.4	953.8
ROAD RUNNER	7845.0	11.5	5640.6	2696.7	9600.0	1491.9	5661.0	8895.1	11730.0
SEAQUEST	42054.7	68.4	683.3	286.9	354.1	240.1	384.5	301.2	550.5
UP N DOWN	11693.2	533.4	3350.3	2847.6	2877.4	2901.7	2955.2	3180.8	3376.3

Table 8: Average episode returns on each of 26 Atari games at 100K training steps, across 4 random runs. In each game, the highest score is bold, where the scores of baseline models are listed in both DrQ and CURL papers. The proposed CCLF demonstrates better overall performance on 8 out of 26 games.

- Data-Efficient Rainbow (Eff. Rainbow) [van Hasselt *et al.*, 2019].
- Efficient DQN [Mnih *et al.*, 2013].
- CURL [Laskin *et al.*, 2020a].
- DrQ [Yarats *et al.*, 2020].

For consistency, we directly use the average scores of all baseline models that are recorded in DrQ and CURL papers. It can be seen from Table 8 that CCLF can improve over CURL and DrQ on 11 and 18 out of 26 games, with about 18% and 39% performance improvements on average respectively. In particular, we have obtained $2.07\times$, $1.66\times$, and $1.65\times$ mean scores than CURL on the Road Runner, Demon Attack, and Alien games. Compared to DrQ, CCLF outperforms it with $2.30\times$, $1.86\times$, and $1.83\times$ mean scores on the Freeway, Hero, and Seaquest games. These results have demonstrated the desired sample-efficient capability of the proposed CCLF. In addition, CCLF even achieves super-human performance on Krull and Road Runner tasks. Although CCLF attains state-of-the-art in 8 games, there are still some gaps, compared to the human performances and the top performing model-based method SimPLe on the other tasks. This shortcoming can also be found in both DrQ and CURL results, where further improvement towards human-level performance is desired.

C.3 Additional Discussion on MiniGrid

As shown in Figure 3 from the main paper, CCLF can significantly improve the sample efficiency as well as the ultimate learning performances, by extending both A2C and RE3 algorithms. In particular, incorporating CCLF directly on A2C is sufficient to outperform RE3 by reaching optimal performance levels faster with even higher scores in all three tasks. Meanwhile, integrating CCLF to RE3 can further improve the sample efficiency. In the DoorKey-8x8 task, our agent started to obtain non-trivial scores at around 700K steps, while conventional A2C has failed even at 2400K step and RE3 started to improve only at around 1200K steps. As RE3 has been empirically proven more effective than other curiosity-driven methods (ICM [Pathak *et al.*, 2017] and RND[Burda *et al.*, 2018]), we can conclude that our CCLF is sample-efficient and is capable of encouraging exploration effectively in the MiniGrid environments.

C.4 Effectiveness of the Proposed Components

One might wonder if the proposed CCLF benefits mainly from one or several curiosity-based components in practice. Hence, we empirically examine the effectiveness of all possible (15) combinations of the proposed four components on the Cartpole task from the DMC suite, averaging by 6 random runs. In this task, agents need to swing up a pole over the cart by continuously moving the cart around.

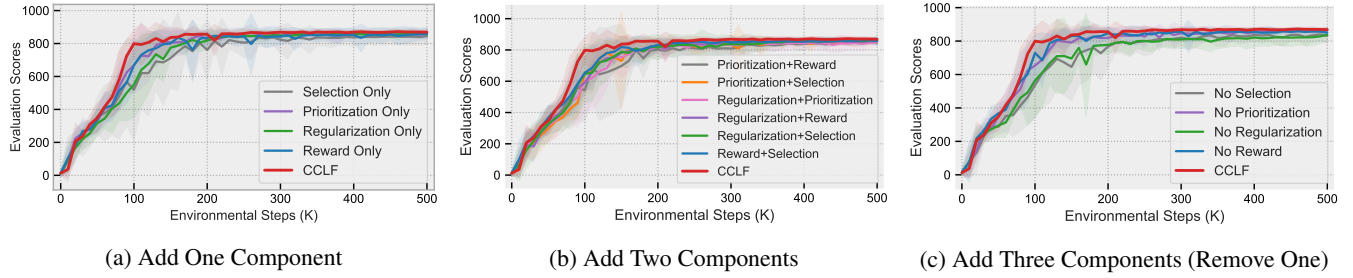


Figure 8: An investigation of the effectiveness of all curiosity-based components on the Cartpole-Swingup task. Adding one component alone or any two components is not sufficient for learning improvement, but instead can cause extra instability and complexity. Removing reward or prioritization has less impact than removing regularization or selection, but it is still less competitive than using all four components.

Adding One Component

We respectively incorporate each curiosity-based component (Selection Only, Prioritization Only, Regularization Only, and Reward Only) into the SAC base algorithm and compare their performances against our full CCLF. It can be observed from Figure 8(a) that all models approximately obtain the same performances at 500K regimes. For the sample efficiency, all four curves are significantly below the proposed CCLF at 100K. Meanwhile, there exists some sudden increase or decrease in the learning curves of all four models, indicating the occurrence of instability. Therefore, each component alone cannot achieve the desired sample efficiency and can even cause unstable learning qualitatively. In contrast, our collaborative CCLF can navigate all components together, which demonstrates effective collaboration.

Model	100K Step Score	500K Step Score
Regularization Only	551 \pm 146	857 \pm 10
Selection Only	561 \pm 181	837 \pm 38
Reward Only	668 \pm 105	858 \pm 27
Prioritization Only	670 \pm 127	858 \pm 16
CCLF	799\pm61	869\pm9

Table 9: Results for the sample efficiency at 100K environment steps and asymptotic performance at 500K environment steps by adding only one proposed component.

In addition, we further compare and analyze the sample efficiency and ultimate performance quantitatively according to the results in Table 9. For the sample efficiency at 100K environment steps, Reward-Only and Prioritize-Only obtain similar performances, which outperform Regularize-Only and Select-Only. However, our proposed CCLF achieves even a $1.19 \times$ mean score at 100K steps compared to the best performance among these four models. Meanwhile, we can observe that the standard deviations of these four models are much higher than our proposed CCLF at both 100K and 500K environment steps. This further implies that each component alone cannot resolve the instability issue that occurred in the learning process. In particular, Select-Only has the highest standard deviation because it selects the most challenging inputs that agents cannot accurately predict for learning. However, as the learning process is not properly adapted to cap-

ture the novel knowledge contained in the selected inputs, the instability issues cannot be avoided. CCLF collaboratively adapts the learning process with all four RL components and therefore its standard deviation is the lowest, where the agents can learn with contrastive curiosity. From the perspective of the ultimate performance, the proposed CCLF is also the best compared to the other four models, indicating an improved learning capability as the result of the efficient collaboration of all RL components as well.

Adding Two Components

Two proposed components are incorporated into the base algorithm in this sub-section. It can be observed from Figure 8(b) that all models approximately obtain the same performances at 500K regimes. For the sample efficiency, all six curves are significantly below the proposed CCLF at 100K. Among the six experimented models, Reward+Selection performs the best while Prioritization+Reward learns the worst. It seems that regularization and selection are more important to attain the desired performance. However, only incorporating these two components (Regularization+Selection) may instead introduce some instability, which should be addressed by the remaining two components as a whole. In contrast, our collaborative CCLF can navigate all components together, which demonstrates effective collaboration.

Model	100K Score	500K Score
Prioritization+Reward	542 \pm 147	848 \pm 12
Prioritization+Selection	655 \pm 104	859 \pm 9
Regularization+Prioritization	601 \pm 137	851 \pm 13
Regularization+Reward	591 \pm 52	857 \pm 12
Regularization+Selection	648 \pm 135	861 \pm 11
Reward+Selection	654 \pm 74	858 \pm 22
CCLF	799\pm61	869\pm9

Table 10: Results for the sample efficiency at 100K environment steps and asymptotic performance at 500K environment steps by adding two proposed components.

Quantitatively, we compare and analyze the sample efficiency and ultimate performance based on the results in Table 10. For the sample efficiency at 100K environment steps, Prioritization+Selection, Regularization+Selection and Reward+Selection obtain similar results, which outperform

the others with Prioritization+Reward being the worst. However, our proposed CCLF achieves even a $1.22\times$ mean score at 100K steps compared to the best performance among these six models. Meanwhile, we can observe that the standard deviations of these models except for Regularization+Reward are much higher than our proposed CCLF at 100K environment steps. It implies that CCLF can stably adapt the learning process by the contrastive curiosity that seamlessly connects all four components.

Adding Three Components

We respectively remove one component from the full CCLF and present the learning performances in Figure 8(c). In particular, removing only prioritization (No Prioritization) or reward (No Reward) only results in a slight downward shift in the learning curves while No Selection and No Regularization show significant performance downgrade in both sample efficiency and learning capabilities. It indicates that all four components are necessarily important to attain state-of-the-art results, where regularization and selection are more important than prioritization and reward.

Model	100K Score	500K Score
No Selection	536 ± 141	832 ± 35
No Prioritization	653 ± 89	863 ± 10
No Regularization	565 ± 161	837 ± 25
No Reward	729 ± 82	859 ± 17
CCLF	799 ± 61	869 ± 9

Table 11: Results for the sample efficiency at 100K environment steps and asymptotic performance at 500K environment steps by adding three (removing one) proposed components.

Quantitatively, we also compare and analyze mean scores at 100K and 500K steps, as shown in Table 11. For the sample efficiency at 100K environment steps, No Selection and No Regularization result in 33% and 29% return decreases compared to the full model; meanwhile, their standard deviations are much higher, indicating the occurrence of instability. Similarly, these two models have caused performance downgrades at even 500K steps, with larger standard deviations as well. As a result, we believe regularization and selection play more important roles in CCLF, but it still requires the four components to work collaboratively to obtain the desired sample efficiency and learning performances.